Patterning of silver on the micro- and nano-scale by local oxidation using air plasma

Abdel-Aziz El Mel, Romain Gautier, Nicolas Stephant, Pierre-Yves Tessier, Yousef Haik

Patterning of silver on the micro- and nano-scale by local oxidation using air plasma

Abdel-Aziz El Mel, Romain Gautier, Nicolas Stephant, Pierre-Yves Tessier, Yousef Haik*

Dr. A. A. El Mel
College of Science and Engineering, Hamad bin Khalifa University, P.O. Box 34110, Doha, Qatar
Institut des Matériaux Jean Rouxel, Université de Nantes, CNRS, 2 rue de la Houssinière B.P. 32229, 44322 Nantes cedex 3, France

Dr. R. Gautier, Mr. N. Stephant, Prof. P. Y. Tessier
Institut des Matériaux Jean Rouxel, Université de Nantes, CNRS, 2 rue de la Houssinière B.P. 32229, 44322 Nantes cedex 3, France

Prof. Y. Haik
College of Science and Engineering, Hamad bin Khalifa University, P.O. Box 34110, Doha, Qatar

Corresponding author
E-mail: Abdelaziz.elmel@gmail.com
Dr. A. A. El Mel
College of Science and Engineering, Hamad bin Khalifa University, P.O. Box 34110, Doha, Qatar
Institut des Matériaux Jean Rouxel, Université de Nantes, CNRS, 2 rue de la Houssinière B.P. 32229, 44322 Nantes cedex 3, France

Keywords: Nanopatterning; micropatterning; thin films; nanowires; silver

A novel low temperature micro- and nano-patterning approach of metal silver thin films is demonstrated. The process involves local deposition of carbon mask created in situ using the e-beam of scanning electron microscope followed by radio frequency air plasma oxidation. We show that by selecting the appropriate experimental conditions, silver can be transformed locally from metallic to nanoporous oxide. Etching the oxide phase in ammonia solution allows obtaining metal silver patterns. We further show that this approach is not limited to thin films but can be rather extended to nanowires which allows creating periodic metal/metal oxide nanojunctions.

1. Introduction

Micro and nanopatterning have strongly contributed to the development of many modern technological areas ranging from microelectronic to biotechnology [1-3]. Due to the rapid increase of nanotechnology and the related research areas that we are witnessing lately, improving the patterning approaches is becoming mandatory. This is related to the fact that each process has its own advantages and limitations. For example, photolithography is a fast process that have strongly served the microelectronic industry but its main drawback is related to the patterns resolution limited by the diffraction law of light [3]. On the other hand, electron beam lithography allows reaching a better resolution but it requires, however, a longer writing time; in addition, it is an expensive technique. Nanolithography using atomic force microscopy is also a powerful approach to create nanopatterns but it is limited by the writing speed of the used probe [4]. According to the application, each one of the existing patterning approaches can be appropriately selected. For this reason, identifying and developing new patterning approaches with new abilities compared to the already existing ones can be of real benefit for many technological applications.

The oxidation of silver by atomic oxygen has been widely studied in the past to avoid the degradation of silver components used in spacecraft navigating in low earth orbit (LEO) [5-7]. The reaction occurring between metal silver and the high density atomic oxygen presents in LEO generated by the decomposition of molecular oxygen by the UV radiations is behind this degradation process [6]. This corrosion effect is well documented in literature and the fundamental mechanisms are well understood [5-17]. Although such an effect was considered in the past as a nuisance for spacecraft applications, we have recently showed it can be used in a beneficial way to create nanoporous nanomaterials [18,19]. It should be mentioned that the

formation of nanoporosity upon oxidation of silver is a very particular phenomenon that cannot be detected in case of other metals. Meanwhile, in case of iron, when oxidized using an after-glow oxygen plasma, one-dimensional (1D) nanostructures can be obtained [20]; the formation of 1D nanostructures was also reported in case of copper when oxidized using thermal oxidations processes [21]. In this communication we report for the first time how such an undesired oxidation effect can be used for the patterning of metal silver thin films on the micro- and/or the nanoscale. Patterning of silver films is an appealing topic for flexible electronic and related areas [22]; among the main applications stands silver-based highly flexible transparent conductive electrodes [23]. Various processes were reported to pattern silver such as direct laser writing [22], optical patterning combined with Langmuir-Blodgett [24], cold-plasma-jet scanning [25] and microreactor-assisted printing [26]. With our process, we used air plasma to oxidize locally silver films through carbon masks created by e-beam deposition *in situ* scanning electron microscope (SEM). We further show how the removal of the created oxide using an ammonia solution allows obtaining arrays of silver structures. For the proof of concept, we show in this paper how to create periodic squares of metal silver structures but the same process can be used to create different shapes such as lines, meshes and grids by using appropriated mask designs. Such structures can be of real interest for flexible electronics as they can be used as flexible transparent conductive electrodes for emerging electronic devices [27]. The concept of local oxidation is further applied to nanowires which allow creating metal/oxide periodic one-dimensional nanojunctions. Such patterned or oxide/metal hybrid structures can be of real interest for many research areas as they combine at the same time the properties of metal silver as well as the ones the nanoporous oxide. Thanks to its great optical properties [28], silver structures can be used to develop SERS-sensors (surface enhanced Raman scattering) to detect

small molecules using light [29]. On the other hand, taking advantage of its high active specific surface area, the nanoporous oxide phase can be used to develop resistive-based sensors with enhanced sensitivity and response time [30].

2. Experimental details

The local oxidation experiments were carried out using a radio-frequency plasma source Evactron® Model 25 De-Contaminator by XEI Scientific, Inc. The load-lock of the scanning electron microscope (SEM) served as the oxidation chamber. Ambient air was used as a feeding gas to generate the plasma and oxidize the silver films and nanostructures. For all the experiments, the distance between the source and the substrate was kept constant at 20 mm. An electrical power of 20 W was used for all the experiments whereas the discharge pressure was fixed at 50 Pa. The room humidity was 45% at 300 K corresponding to a water partial pressure of about 1%. The wet etching of Ag_2O was carried out with a solution of NH_3 30% during one hour. The carbon mask deposition was performed in situ SEM using the e-beam. We took benefits of the carbon contamination triggered by the exposure of the films to the e-beam in order to deposit locally carbon on a specific area. To perform the deposition, the electron beam was focused on a selected area by increasing the magnification of the SEM. During exposure, the hydrocarbon contamination present on the extreme surface of the silver film due to its exposure to atmosphere, burns and transforms to a hard carbon layer. According to the exposure time the size and the thickness of the carbon mask can be defined, respectively. The average deposition rate of carbon at the center of the exposed are was around 25 nm/min. All carbon depositions were carried out using the e-beam with an acceleration voltage of 5 kV using the slowest scanning speed available with our SEM and without changing other conditions compared to those used for images.

To measure the thickness of a metal silver pattern at the end of the process we used the stereoscopy acquisition technique [31] in situ SEM. Three images of the same patterned area were acquired for three values of sample tilt (0°, 7° and 15°). With those images we calculated an elevation distance map (EDM) with the MEX metrology software (ALICONA *Imaging GmbH Graz, Austria)*, and then we extracted a line profile along the pattern to visualize its shape and measure its thickness.

3. Results and discussion

3.1. Patterning of thin films

The patterning approach developed in this work is based on the local oxidation of silver films through carbon mask using air plasma. As illustrated in Figure 1, the approach requires depositing a silver thin film at first (Figure 1a). We used magnetron sputtering to deposit the films, but any other process allowing obtaining uniform coating over the substrate can be used. It is important to mention that the thickness of the film should not exceed 100 nm otherwise the oxidation process becomes more difficult to perform. In here the thickness of the silver film was fixed to 100 nm. In the second stage the carbon features, serving as a mask to protect silver against oxidation, are then created on top of the silver film using e-beam *in situ* SEM (Figure 1b). The deposition process of the carbon mask is described in details in the experimental section. Note that the mask can be created by any lithography process and various materials can be also used as a mask.

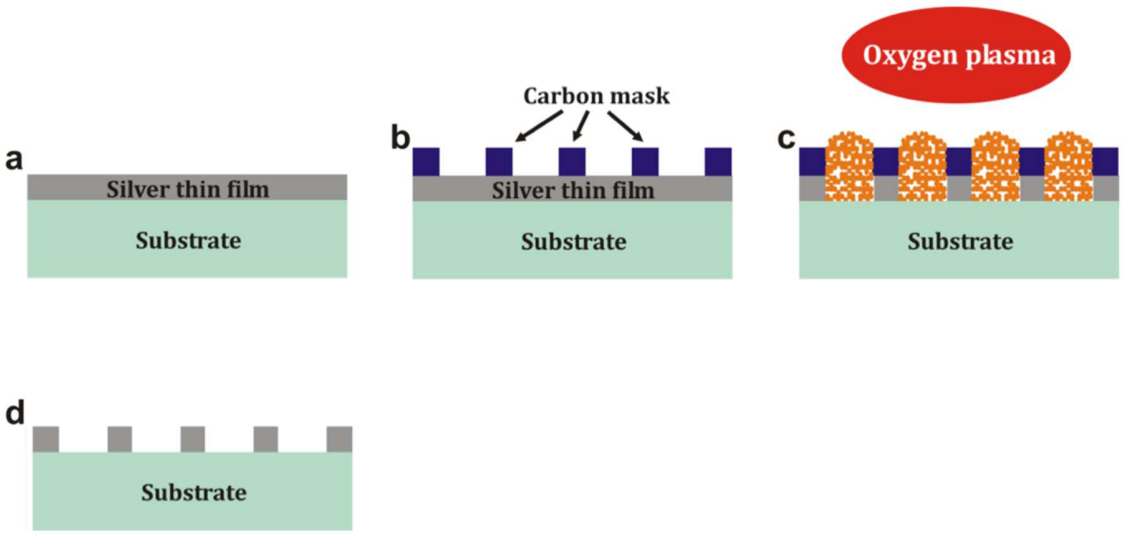

Figure 1: Schematic illustration showing the different steps of the patterning approach developed in this work. a) Deposition of silver film, b) fabrication of the carbon mask using the e-beam *in situ* SEM, c) local oxidation of the silver film through the carbon mask using radio-frequency air plasma, d) formation of metal silver patterns after removal of silver oxide in ammonium solution.

After creating the carbon features, the silver film is exposed to a radiofrequency air plasma through the carbon mask (Figure 1c). This step allows transforming the metal silver exposed locally to the air plasma into nanoporous silver oxide that can be dissolved later on using ammonia solution (Figure 1d). The size of the silver patterns is dependent to many parameters including i) the dimensions of the carbon features playing the role of a mask, ii) the oxidation time, as well as iii) the etching time of Ag_2O in the ammonium solution.

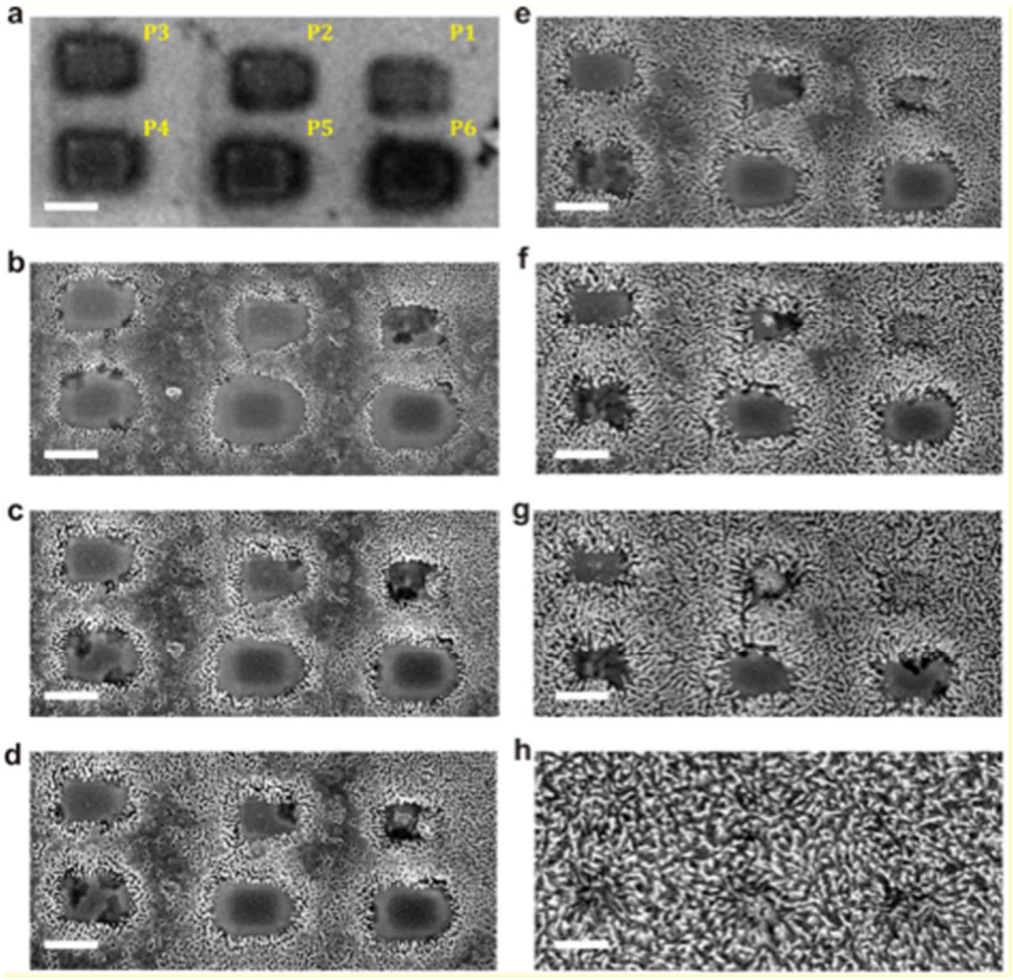

Figure 2: Before oxidation: a) P1-P6 represents the spots exposed to carbon for various durations: P1: 1 min, P2: 2 min, P3: 3 min, P4: 4 min, P5: 5 min, P6: 6 min. After oxidation: b) 3 min, c) 4 min, d) 5 min, e) 6 min, f) 8 min, g) 10 min, h) 25 min. Scale bar: 500 nm.

As a first step, the thickness of the carbon mask used to protect some specific regions of the silver film from the plasma need to be optimized. We therefore considered the series of experiments presented in Figure 2 where the deposition time of the carbon mask was tuned. The regions exposed to the e-beam for different durations are denoted P1, P2, etc… the exposure time varied from 1 min (P1) to 6 min (P6). The oxidation conditions were selected based on our previous work [11,12]; in such oxidations conditions Ag_2O phase can be formed. As it can be

seen, after 3 min of oxidation a slight nanoporosity starts appearing on the surface of the unprotected areas of the film whereas the areas covered with carbon remain unchanged (Figure 2b). Increasing the oxidation time to 4 min (Figure 2c) increase the degree of nanoporosity in the unprotected areas; considering the regions protected with the carbon mask, a lateral grow of oxide at the edges of the masks can be noticed leading in the decrease of the surface of the protected areas. This can be related to the diffusion of silver from the regions located under the carbon mask toward the upper surface exposed to the plasma similar to the mechanism proposed by Yu et al. in case of nanowires exposed to atomic oxygen [11]; as a consequence, an oxide phase starts growing laterally which reduces the dimensions of the carbon mask. In parallel to this diffusion, one must consider the etching of the carbon mask by the air plasma during the treatment. As the carbon mask is expected to be thinner on the edges compared to the centre region due to the nature of the deposition process, the oxidation is expected to be more efficient on the edges of the carbon mask compared to the centre where the carbon film is thicker. When reaching 5 min of oxidation (Figure 2d), the nanoporosity becomes more pronounced for the unprotected areas of the film. When examining the mask regions, it can be noticed that for P1 (area with 1 min of carbon deposition) a morphological change starts occurring for the whole area are including the edges and the centre region. This indicated that a carbon deposition of 1 min is not enough to protect the silver surface against an oxidation treatment of 5 min. We can also notice that the surface of the other carbon-protected regions P2-P6, the diameter of the areas reduces due to the lateral oxidation occurring at the edges as explained for the previous condition (i.e. 4 min of oxidation). For 6 min of oxidation time (Figure 2e), while P2-P6 still being able to resist the oxidation process, the carbon at P1 completely disappears and nanoporous silver oxide forms in place. Further increasing the oxidation time to 8 min results in the increase of

nanoporosity of the material; it can be also noticed that the P1 mask has completely disappeared (Figure 2f). When reaching 10 min (Figure 2g), As for P1, the area protected by P2 also becomes nanoporous while the diameter of the rest of the carbon masks (i.e. P3-P6) keeps shrinking. Interestingly, for this condition one can remark that the unprotected area of the film become fully nanoporous. For a long oxidation duration of 25 min, in addition to the fact that the film becomes fully nanoporous, the carbon masks completely disappear (Figure 2h). As a conclusion to this series of experiments, to transform a film to nanoporous while protecting some specific regions on the surface, the carbon deposition time should be at least 3 min which correspond to P3. However, one must take into account the shrinkage of the carbon mask and thus it would be more suitable to use a carbon deposition of 6 min if the purpose is to keep the dimension of the protected area unchanged by the end of the oxidation process. However, the lateral decrease of the area of the carbon mask can be used in a beneficial way to control the size of the non-oxidized region. This is demonstrated in Figure 3 where a carbon feature was created using 4 min of carbon deposition and then the specimen was exposed to air plasma. Increasing the oxidation time from 1 to 4 min allows decreasing the size of the silver pattern to roughly 200 nm (Figure 3a-d).

After identifying the optimal conditions of our local oxidation process, we applied lift-off to create metal silver nanopatterns as shown in Figure 4a and 4b. To obtain these patterns, the created oxide was dissolved in ammonia solution. The treatment conditions are explicitly described in the experimental section. The created patterns are ~1500 nm in width and ~900 nm in height. It should be noted that reaching smaller dimensions is more challenging due to the delamination issue encountered during the treatment in the ammonia solution. However, one must take in consideration that adding an adhesion layer (e.g. titanium or chromium) may allow

overcoming this issue but after the liftoff one will end up with silver patterns created on top a metal-coated substrate instead of patterns directly fabricated on the substrate which can be a limiting factor for some applications. One can also remark that even after a long treatment in the ammonia solution, some undesired oxide residue remains present on the edges of the silver pattern (Figure 4a and 4b).

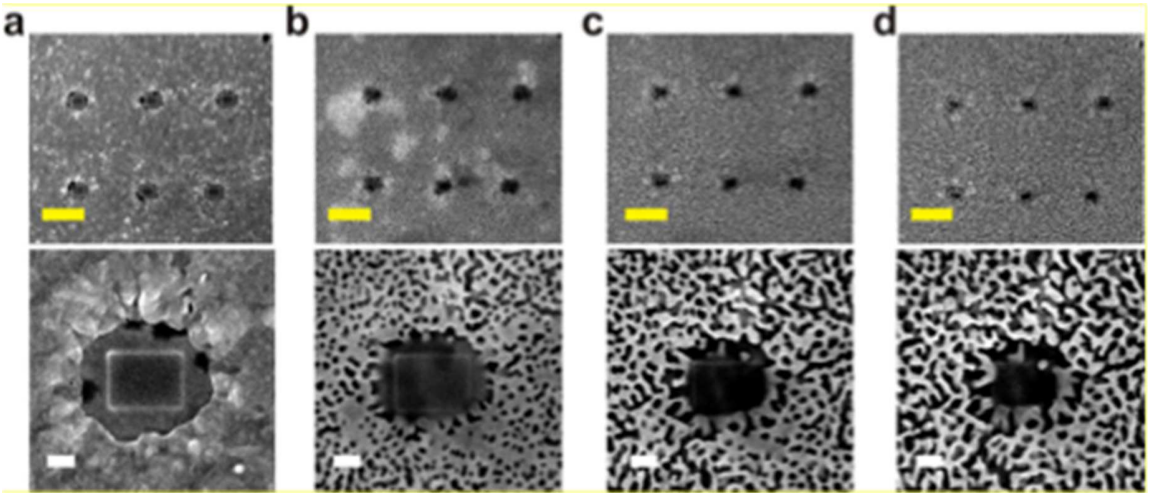

Figure 3: SEM images of a silver film with six carbon features, deposited for 4 min, used as a mask and oxidized for: 1 min, 2 min, 3 min and 4 min. Yellow scale bar: 1 micron; White scale bar: 100 nm.

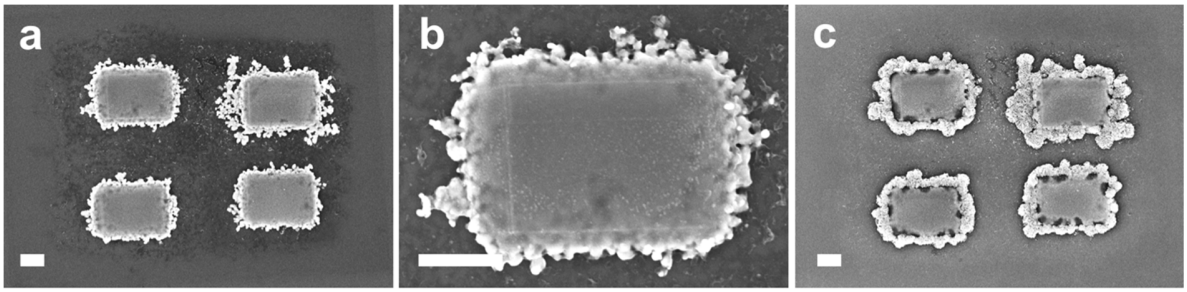

Figure 4: (a) low and (b) high-resolution SEM images of a silver nanopatterns created by plasma oxidation of 100 nm thick silver film covered with four carbon features followed by the removal of the oxide phase in ammonia solution. The deposition time of the carbon mask was fixed to 6

min whereas the oxidation time was 6 min. (c) Silver/silver oxide complex features created by exposing the silver patterns shown in panel a to air plasma for 30 s. Scale bar: 500 nm.

To check the quality of the silver features, SEM-EDS mapping was performed on a feature after processing (Figure 5). As it can be seen, the feature is mainly constituted of metallic silver. One can also notice the presence of carbon residue on top of the silver feature. As the carbon mask is still present on the top surface of the created silver patterns, an additional oxidation treatment of the created silver patterns can lead to more complex metal/oxide nanopatterns defined by the metal silver rectangles surrounded by an oxide frame (Figure 4c).

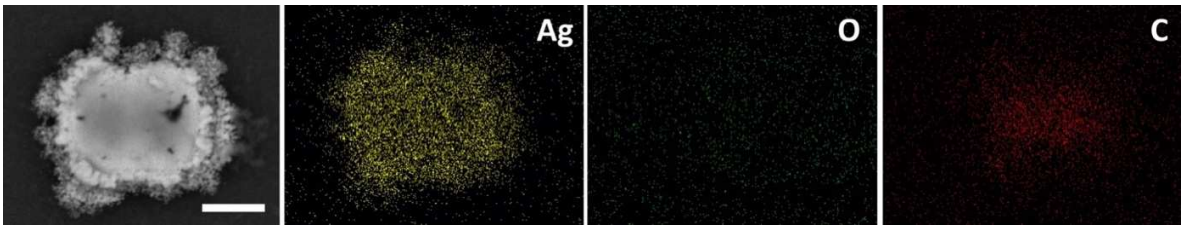

Figure 5: SEM-EDS mapping showing the elemental distribution of silver, oxygen and carbon in a feature after processing. Scale Bar: 1µm.

To determine the thickness of the pattern we performed a stereoscopic acquisition and evaluated the thickness variation along the red scan-line profile shown in Figure 6. As it can be seen, the thickness of the feature is nearly the same as the original silver layer (100 nm).

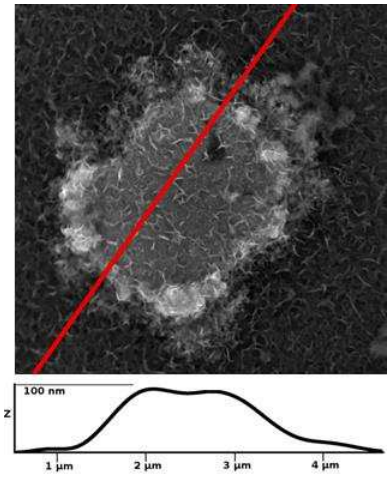

Figure 6: Line profile extracted from stereoscopic SEM acquisition of silver pattern created using our process. The height of silver pattern is about 100 nm which correspond to the initial thickness of the silver layer.

3.2. Metal/Metal oxide nanojunctions

The concept of local oxidation developed so far is not limited to thin films but can be rather extended to one-dimensional nanostructures. In Figure 7 it is shown how the local oxidation process can be applied to a silver nanowire to create metal/metal oxide periodic nanojunctions. As it can be seen, when a silver nanowire (Figure 7a) is exposed to the e-beam in situ SEM, a carbon layer grows instantly on its surface (Figure 7b). The growth of this carbon layer was much faster than in case of thin films. It can be noticed that this layer is able to protect the silver nanowire from plasma oxidation (Figure 7c). Taking advantage from such an effect, it is possible to oxidize periodically specific region of the silver nanowire on the nanoscale allowing obtaining metal/oxide nanojunctions (Figure 7d).

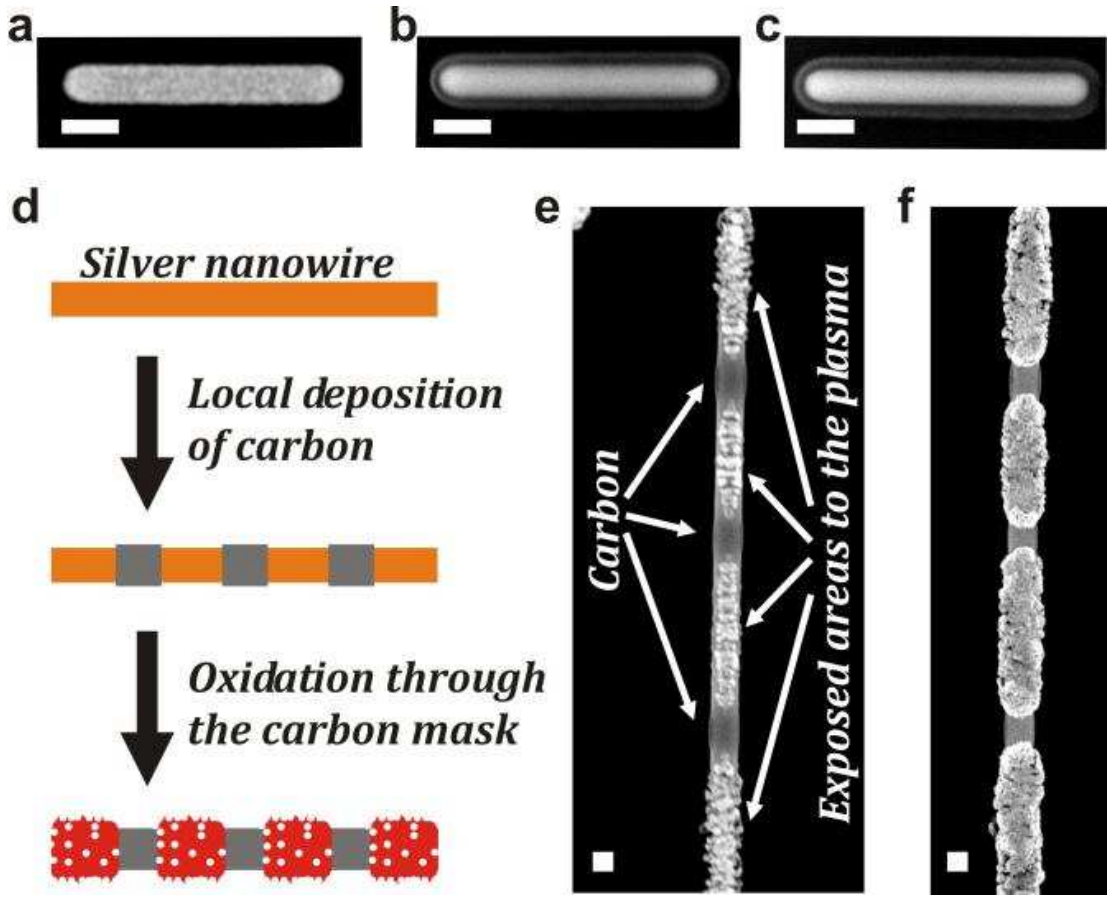

Figure 7: Concept of the nanopatterning process using local oxidation of silver nanowires by atomic oxygen. SEM images of a silver nanowire (a) before and (b) after deposition of carbon under electron beam in the SEM for 30 s. (c) SEM image of the silver nanowire with deposited carbon shown in panel b after exposure for 1 min to the air plasma operating at 20 W and 50 Pa. (d) Scheme of the approach followed to oxidize locally the nanowires and create periodic silver/silver-oxide nanojunctions. SEM image of a silver nanowire oxidized through a carbon mask for: (e) 30 s and (f) 60 s. Scale bar: 100 nm.

As it can be seen, for 30 s of oxidation of a silver nanowire covered with periodic carbon features, similarly to the case of silver thin films, silver oxide nanograins start growing at the unprotected areas (Figure 7e). Increasing the oxidation time to 60 s allows transforming the regions exposed to the plasma into nanoporous silver oxide (Figure 7f).

4. Conclusion

An original patterning approach of silver films was demonstrated. The approach involves the deposition of carbon mask in situ SEM, the oxidation of silver using air plasma, and the removal of the oxide phase in ammonia solution. To successfully create silver patterns, the carbon mask and oxidation conditions must be carefully selected. We further showed that by applying an additional oxidation step to the created silver patterns covered by carbon results in the formation of silver features surrounded by oxide frames. Furthermore, we showed that our process is not limited to thin films but can be rather extended to silver nanowires allowing creating metal/oxide one-dimensional nanojunctions. Our approach paves the way for many applications such as the creation of silver substrates for surface enhanced Raman scattering (SERS) sensors or gas sensors based on metal/oxide hybrid micro- and nano-materials.

References

[1] Xia, Y.; Whitesides, G. M.; *Annu. Rev. Mater. Sci.,* **1998,** *28,* 153-84.

[2] Kim, P.; Kwon, K. W.; Park, M. C.; Lee, S. H.; Kim, S. M.; Sub, K. Y.; *Bochip Journal*, **2008**, *2*, 1-11.

[3] Xia, Y.; Whitesides, G. M.; *Angew. Chem. Int. Ed.*, **1998**, *37*, 550-575.

[4] Zheng, J.; Chen, Z.; Liu, Z.; *Langmuir*, **2000**, *16*, 9673–9676. M. L. Zheludkevich, 5. Gusakov, A. G.; Voropaev, A. G.; Vecher, A. A.; Kozyrski, E. N.; Raspopov, S. A.; *Oxid. Met.*, **2004**, *61*, 39-48.

[6] Rooij, A. D.; *ESA J.*, **1989**, *13*, 363.

[7] Reddy, M. R; *J. Mater. Sci.*, **1995**, *30*, 281-307.

[8] Osborne, J. J.; Harris, I. L.; Roberts, G. T.; Chambers, A. R.; *Rev. Sci. Instrum.* **2001***, 72,* 4025-4041.

[9] Zheludkevich, M. L.; Gusakov, A. G.; Voropaev, A. G.; Vecher, A. A.; Kozyrski, E. N.; Raspopov, S. A.; *Oxid. Met.* **2004**, 61, 39-48.

[10] Zheludkevich, M. L.; Gusakov, A. G.; Voropaev, A. G.; Vecher, A. A.; Kozyrski, E. N.; Raspopov, S. A.; *Protection of Materials and Structures from Space Environment* **2003**, 5, 351-358.

[11] Yu, L.; Yan, Z.; Cai, Z.; Zhang, D.; Han, P.; Cheng, X.; Sun, Y.; *Nano Lett.* **2016**, *16*, 6555-6559.

[12] Li, Y.; Zhang, Y.; Fu, H.; Wang, Z.; Li, X; *Mater. Lett.* **2014**, *126*, 131-134.

[13] Waterhouse, G. I. N.; Bowmaker, G. A.; Metson, J. B.; *Appl. Surf. Sci.* **2001**, *183*, 191-204.

[14] Edwards, D. L.; Williams, J. R.; Fromhold, A. T.; Barnes, P. A.; Wey, J. P.; Neely, W. C.; Whitaker, A. F.; *Nucl. Instrum. Methods Phys. Res. Sect. B*, **1993**, *79*, 676–679.

[15] Li, L.; Yang, J. C.; Minton, T. K.; *J. Phys. Chem. C*, **2007**, *111*, 6763-6771.

[16] Moore, W. M.; Codella, P. J.; *J. Phys. Chem.*, **1988**, *92*, 4421-4426.

[17] Banks, B. A.; Miller, S. K. R.; de Groh, K. K.; Demko, R.; *NASA/TM*, **2003**, 212484.

[18] El Mel, A. A.; Stephant, N.; Hamon, J.; Thiry, D.; Chauvin, A.; Chettab, M.; Gautron, E.; Konstantinidis, S.; Granier, A.; Tessier, P. Y.; *Nanoscale*, **2016**, *8*, 141-148.

[19] El Mel, A. A.; Stephant, N.; Molina-Luna, L.; Gautron, E.; Haik, Y.; Tabet, N.; Tessier, P. Y.; Gautier, R.; *J. Phys. Chem. C*, **2017**, *121*, 19497-19504.

[20] A. Imam, T.Gries, H.Sezen, M.Amati, D.Mangin, T.Belmonte. Nano-structures & Nano-objects 7 (2016), 41-48

[21] J. Hilman, A. Yost, J. Tang, B. Leonard, T. Chien. Nano-structures & Nano-objects 11 (2017), 124-128

[22] Liu, Y. K.; Lee, M. T.; *ACS Appl. Mater. Interfaces* **2014**, *6*, 14576–14582

[23] Cho, E. H.; Hwang, J.; Kim, J.; Lee, J.; Kwak, C.; Lee, C. S.; OPTICS EXPRESS **2015**, *23*, 26095.

[24] Kim, H.; Shin, H.; Ha, J.; Leea, M.; *J. App. Phys.* **2007**, *102*, 083505.

[25] Liu, L.; Li, H. Y.; Ye, D.; Yu, Y.; Liu, L.; Wu, Y.; *Nanotechnology* **2017**, *28*, 225301.

[26] Choi, C. H.; Allan-Colea, E; Chang C.H. ***J. Mater. Chem. C***, **2015**, ***3***, 7262-7266.

[27] Yi, P.; Zhang, C.; Peng, L.; Lai, X. *RSC Advances* **2017**, *7*, 48835-48840.

[28] X. Jie, N. Bao, B. Gong, S. Zhou. Nano-structures & Nano-objets 12 (2017), 98-105.

[29] M. Sakir, S. Pekdemir, A. Karatay, B. Küçüköz, H. H. Ipekci, A. Elmali, G. Demirel, and M. S. Onses. ACS Appl. Mater. Interfaces 9 (2017) 39795–39803.

[30] A. dey. Mater. Sci. Eng. B 229 (2018) 206-217.

[31] F. Marinello, P. Bariani, E. Savio, A. Horsewell, L. De Chiffre. Critical factors in SEM 3D stereo microscopy. Measurement Science and Technology 19 (2008), 065705.